IEEE Photonics Journal
An IEEE Photonics Society Publication

Open Access

Dynamic Distributed Brillouin Optical Fiber Sensing Based on Dual-Modulation by Combining Single Frequency Modulation and Frequency-Agility Modulation

Volume 9, Number 3, June 2017

Dexin Ba
Dengwang Zhou
Benzhang Wang
Zhiwei Lu
Zhigang Fan
Yongkang Dong, *Member, IEEE*
Hui Li

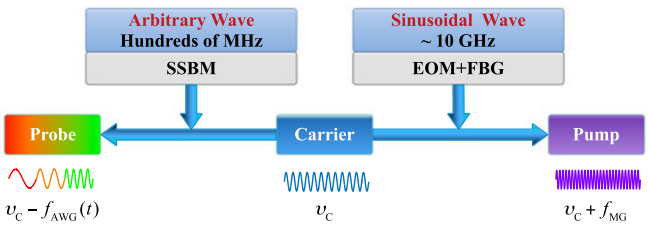

DOI: 10.1109/JPHOT.2017.2690319
1943-0655 © 2017 IEEE

IEEE photonics SOCIETY

IEEE

Dynamic Distributed Brillouin Optical Fiber Sensing Based on Dual-Modulation by Combining Single Frequency Modulation and Frequency-Agility Modulation

Dexin Ba,[1] Dengwang Zhou,[1] Benzhang Wang,[1] Zhiwei Lu,[1] Zhigang Fan,[2] Yongkang Dong,[1] *Member, IEEE*, and Hui Li[3]

[1]National Key Laboratory of Science and Technology on Tunable Laser, Harbin Institute of Technology, Harbin 150001, China
[2]Research Center for Space Optical Engineering, Harbin Institute of Technology, Harbin 150001, China
[3]School of Civil Engineering, Harbin Institute of Technology, Harbin 150001, China

DOI:10.1109/JPHOT.2017.2690319

Manuscript received February 14, 2017; revised March 25, 2017; accepted March 28, 2017. Date of publication March 31, 2017; date of current version April 19, 2017. This work was supported in part by the 863 Program of China under Grant 2014AA110401; in part by the National Key Technology Research and Development Program of the Ministry of Science and Technology of China under Grant 2014BAG05B07; in part by the National Key Scientific Instrument and Equipment Development Project under Grant 2013YQ040815; in part by the National Natural Science Foundation of China under Grant 61575052, Grant 61308004, and Grant 61605034; in part by the Fundamental Research Funds for the Central Universities under Grant HIT.NSRIF.2015041; in part by the China Postdoctoral Science Foundation under Grant 2016M591531; in part by the National Key Laboratory Funds for National Key Laboratory of Science and Technology on Tunable Laser; and in part by the Postdoctoral Foundation of Heilongjing Province under Grant LBH-Z15076. Corresponding author: Y. Dong (e-mail: aldendong@gmail.com).

Abstract: Dynamic Brillouin optical fiber sensors based on fast scanning of Brillouin gain spectrum (BGS) are one of the most promising techniques to measure dynamic strains, where an ~11-GHz bandwidth arbitrary waveform generator (AWG) or a vector microwave generator is essential for frequency agility. A dynamic Brillouin optical fiber sensor based on dual-modulation is proposed here, which aims to realize dynamic sensing via a low-bandwidth AWG. In this protocol, the scanning of BGS is implemented by the combination of a single-frequency modulation and a frequency-agility modulation. The frequency of the single-frequency modulation is slightly lower than the Brillouin frequency shift of the fiber under test so that the tuning range of the frequency-agility modulation is required to cover only several-hundred MHz for the scanning of the BGS, which significantly reduces the bandwidth requirement for the AWG. In experiment, an 11.8-Hz strain is measured with a 30-m fiber, where the spatial resolution and the sampling rate are 1 m and 200 Hz, respectively. Furthermore, by tracking the damping vibration of the optical fiber, its resonant frequency is measured with a sampling rate of 100 Hz.

Index Terms: Brillouin optical fiber sensor, dynamic measurement, frequency-agility, strain measurement

1. Introduction

The techniques of Brillouin optical fiber sensors have attracted much attention for the last 20 years due to the distributed measurements for both strain and temperature [1]–[4]. Traditional Brillouin optical time-domain analysis (BOTDA) protocols are based on the reconstruction of the Brillouin gain spectrum (BGS) to measure the Brillouin frequency shift (BFS) by sweeping the frequency difference between the pump and the probe waves. Due to the comparatively slow-velocity scanning of frequencies, these protocols cannot measure rapidly changing strains, or so-called dynamic strains. In order to solve this problem, various techniques on dynamic Brillouin sensing have been proposed in recent years [5]–[11]. Bernini proposed a "slope-assisted" Brillouin sensing method, which doesn't involve the scanning of the BGS. By setting the frequency difference between the pump and the probe at the middle of the slope of the BGS, the change of the BFS can be detected by measuring the gain variation of the probe [6], [12], [13]–[16]. Its measurement range is determined by the width of the BGS, which limits its application. Since 2003, Hotate's group has proposed several dynamic sensing techniques based on Brillouin optical correlation-domain analysis (BOCDA), in which the fast scanning of the BGS was realized by the direct current modulation of the laser source and a maximum sampling rate of 1000 Hz was attained for single point sensing [17]–[19]. An idea of using Brillouin optical correlation-domain reflectometry (BOCDR) to realize fast sensing was proposed by Mizuno [20], where a strain sampling rate of up to 100 kHz at an arbitrary position was experimentally verified by detecting locally applied dynamic strain at 1 kHz [21]. Remarkably, Peled proposed a dynamic BOTDA based on a frequency-agility technique, with which a 100-Hz strain was measured over a 100-m fiber [7]. The frequency-agility technique is based on an arbitrary waveform modulation, which requires ~11-GHz frequency-agility waveforms for silica fibers. In order to lower the bandwidth requirement of the arbitrary waveform generator (AWG), our group proposed a frequency-agility technique based on second-order sideband modulation, with which an 11-GHz frequency-agility waveform was generated by a 5.5-GHz arbitrary waveform [22]. Using the same frequency-agility technique, a multi-slope assisted BOTDA was proposed by our group, which solved the problem of narrow measurement range in slope-assisted sensors. In experiment, a maximum strain variation up to 5000 $\mu\varepsilon$ was measured in a 32-m Polarization-maintaining (PM) fiber [23].

Frequency-agility is one of the most crucial techniques in dynamic distributed Brillouin sensors, for both BGS-scanning methods and multi-slope-assisted methods. As mentioned above, in order to cover the range of the BGS, the bandwidth of the frequency-agility waveform should be up to ~11 GHz. However, it is very difficult to find an available commercial AWG with such a broad bandwidth. In Peled's scheme, the 11-GHz frequency-agility waveform was generated via a vector signal generator, which shifted the frequency of a several-hundred-MHz arbitrary waveform up to 11 GHz [7]. In the second-order sideband modulation, the bandwidth requirement was reduced by half to 5.5 GHz. In this paper, a frequency-agility method based on dual-modulation is proposed, which can significantly reduce the bandwidth requirement for the AWG to several-hundred MHz. Using this method, distributed measurements of a periodically varied strain and a damping vibration of the fiber are demonstrated.

2. Dual-Modulation

The schematic illustration of the dual-modulation is shown in Fig. 1. Both the pump and the probe waves derive from the same laser source (denoted as carrier in this figure). One part of the carrier is amplitude-modulated with a single-frequency sinusoidal wave to generate the first-order sidebands. The frequency of the sinusoidal wave (denoted as f_{MG}) is ~10 GHz for silica fibers, which is slightly lower than the BFS of the FUT without strain. The first-order sidebands are filtered by a fiber Bragg grating (FBG), keeping only the upper band, which plays the role of the pump wave in the sensor. The other part of the carrier is modulated with a frequency-agility waveform, the frequency of which satisfies

$$f_{AWG}(t) = f_0 + [t/T]\,\Delta f \tag{1}$$

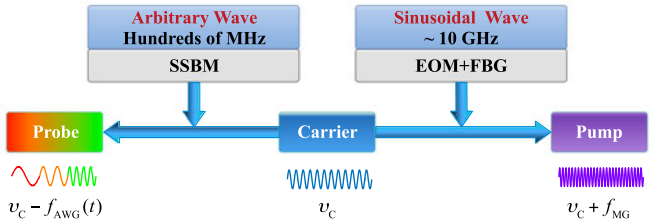

Fig. 1. Schematic illustration of the frequency-agility based on dual-modulation.

where $[x]$ represents the integer part of x. The frequency variation and the time duration of each step are denoted as Δf and T, respectively. The spectrum of the lower first-order sideband comprises of several tones with an interval of Δf. Therefore, the frequency difference between the pump and probe is tuned from $f_{MG} + f_0$ to $f_{MG} + f_0 + [t/T]\Delta f$. Because f_{MG} is quite close to the BFS of the FUT, the bandwidth requirement for the AWG can be reduced to hundreds of megahertz.

Because the scale of $f_{AWG}(t)$ is only several-hundred megahertz, it is impossible to find an optical filter with so narrow bandwidth to suppress the carrier and the upper sideband, which means that it is infeasible to use the scheme of EOM+FBG to obtain the lower first-order sideband. Here, a single-sideband modulator (SSBM) is utilized to generate only the lower sideband. Theoretically, when the RF signals loaded on the two internal Mach–Zehnder interferometers of an SSBM are, respectively, $x\cos(2\pi f_m t)$ and $x\sin(2\pi f_m t)$, by adjusting the voltages of the DC supplies, the lower first-order sideband can be generated together with a negligible upper third-order sideband. Because of the limitation of the extinction ratios of the inner interferometers and the adjusting uncertainties of the DC voltages, it is hard to fully suppress the carrier as well as a few other sidebands. In order to study the influence of these noise tones on the measurement of the BGS, a theoretical model of the dual-modulation-based BOTDA is established. Generally, the residual carrier is the main source of the noise tones, so a residual carrier is introduced into the model as noise tone. Supposing that a probe wave is injected into the FUT at $z = 0$ together with the residual carrier, the optical field can be described as

$$E(t, z) = E_{S0}\exp[j(2\pi\upsilon_S t + \varphi_{S0} - k_S z)] + E_{C0}\exp[j(2\pi\upsilon_C t + \varphi_{C0} - k_C z)] \tag{2}$$

where $E_{S0}(E_{C0})$ is the amplitude of the probe (carrier), $\upsilon_{S0}(\upsilon_{C0})$ is the frequency of the probe (carrier), $\varphi_{S0}(\varphi_{C0})$ is the phase of the probe (carrier), and $k_{S0}(k_{C0})$ is the wavenumber of the probe (carrier). A pump pulse is injected into the FUT at the other end of the FUT (denoted as $z = L$) when $t = T_d$. The echo optical field (including the carrier and the amplified probe) at $z = L$ satisfies

$$\begin{aligned} E_{echo}(T_d + \Delta t) = {} & E_{S0}\exp\left[g_B\left(\upsilon_S, L - \frac{\Delta t}{2n}c\right)\right] \\ & \times \exp\left\{j\left[2\pi\upsilon_S(T_d + \Delta t) + \varphi_{S0} - k_S L + \varphi_B\left(\upsilon_S, L - \frac{\Delta t}{2n}c\right)\right]\right\} \\ & + E_{C0}\exp\{j[2\pi\upsilon_C(T_d + \Delta t) + \varphi_{C0} - k_C L]\} \end{aligned} \tag{3}$$

where g_B and φ_B are the Brillouin gain and phase shift, respectively. Correspondingly, the intensity of the echo trace satisfies

$$I(T_d + \Delta t) = I_{S0}\exp\left[2g_B\left(\upsilon_S, L - \frac{\Delta t}{2n}c\right)\right] + I_{C0} + I_{Beat} \tag{4}$$

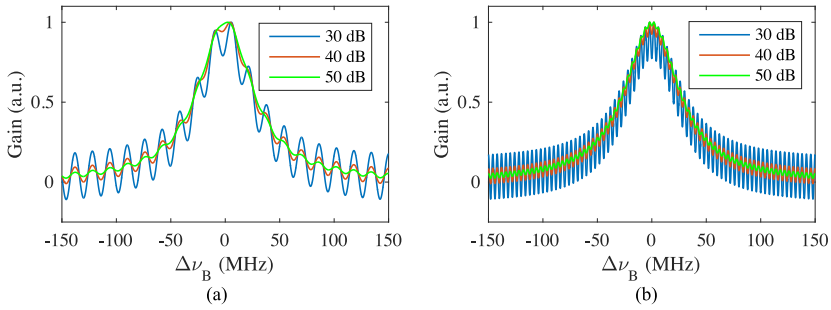

Fig. 2. Modulation on the profile of the BGS introduced by the beat between the probe and the residual carrier. The relative intensities of the residual carrier are 30 dB, 40 dB, and 50 dB less than those of the probe, respectively. (a) $z = (7/8)L$. (b) $z = L/2$.

where $I_{S0} = |E_{S0}|^2$; $I_{C0} = |E_{C0}|^2$. The intensity of the beat signal follows

$$I_{Beat} = 2E_{S0}E_{C0}\exp\left[g_B\left(\upsilon_S, L - \frac{\Delta t}{2n}c\right)\right] \times \cos\left[2\pi\left(T_d + \Delta t - \frac{nL}{c}\right)(\upsilon_S - \upsilon_C) + \varphi_B\left(\upsilon_S, L - \frac{\Delta t}{2n}c\right) + \varphi_{S0} - \varphi_{C0}\right]. \quad (5)$$

Let's consider one point in the FUT, i.e., $T_d + \Delta t - nL/c$ is constant in (5). Therefore, the value of I_{Beat} changes with $\upsilon_S - \upsilon_C$, whose value varies when the BGS is scanned. As a result, a modulation is imposed on the measured profile of the BGS. The modulation "frequency" is

$$|T_d + \Delta t - nL/c| = |T_d + nL/c - 2nz/c| \quad (6)$$

which is the function of z and varies with the position along the FUT. Because BGS is the function of frequency, the unit of the modulation "frequency" is not Hz but second. The difference of the modulation frequencies between different positions is equal to the corresponding time difference in the amplified probe trace.

Using the model, a simulation is carried out to analyze the influence of the residual carrier on the measurement of the BGS. During the simulation, we assume the length of the optical paths of the probe and the pump waves are identical. T_d is set to be nL/c, which guarantees that the probe covers all the FUT before the pump goes into it. The length of the FUT is set to be 50 m and n is chosen to be 1.5. The simulation results are shown in Fig. 2. Fig. 2(a) presents the BGS at $z = (7/8)L$, where the extinction ratio changes from 30 dB to 50 dB. As analyzed above, a sinusoidal modulation is imposed on the profile of the BGS. The modulation frequency can be read to be 62.5 ns. For comparison, the BGS at $z = L/2$ is shown in Fig. 2(b), where the modulation frequency is 250 ns. The difference of the modulation frequencies between the two positions is 187.5 ns, which is equal to the time difference in the echo trace. The results confirm with (6).

It is clear that the modulation can introduce measurement error in Brillouin sensing, especially for the slope-assisted methods, which strongly rely on the profile of the BGS. The simulation implies that the modulation cannot be neglected even when the extinction ratio is up to 50 dB, which is hard to achieve for a commercial SSBM. Though optical methods are impossible to remove the modulation, electrical methods can be employed to suppress it. The analysis above shows that the modulation derives from the beat between the probe wave and noise tones. Its frequency is equal to the multiples of $f_{AWG}(t)$, which is larger than f_0. It means that a low-pass filter can be used to filter out the beat, and ultimately suppress the modulation.

3. Experiments and Results

The experimental setup for dynamic sensing based on dual-modulation is shown in Fig. 3. A 1550-nm fiber laser with 40-kHz linewidth was divided by a 3-dB coupler for providing the pump and

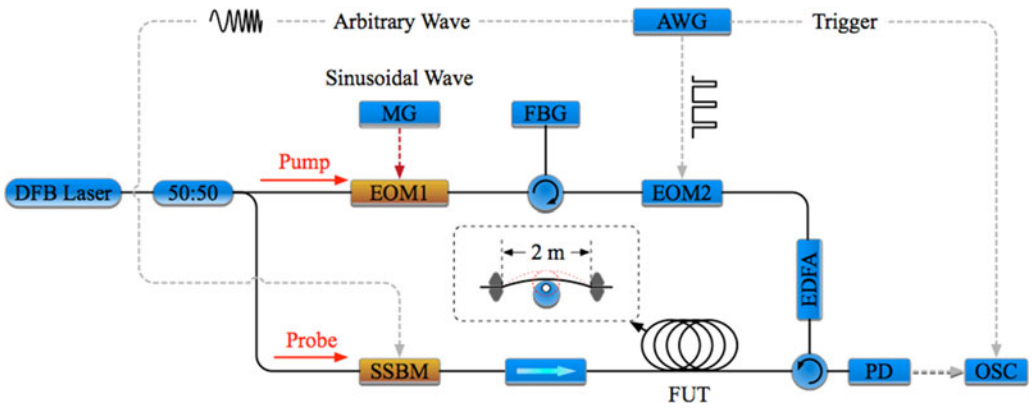

Fig. 3. Experimental setup of dynamic Brillouin sensing based on dual-modulation. MG: microwave generator, EOM: electro-optic modulator, SSBM: single-sideband modulator, FBG: fiber Bragg grating, EDFA: erbium doped fiber amplifier, FUT: fiber under test, AWG: arbitrary waveform generator, PD: photodetector, OSC: oscilloscope.

the probe waves. One of the coupler's outputs, serving as the pump, was modulated by an intensity modulator (EOM1) which worked at the carrier suppression mode. The output of EOM1 was filtered by a fiber Bragg grating (FBG) to retain the upper first-order sideband. It was then modulated to 10-ns pulses by EOM2. After being amplified by an erbium doped fiber amplifier (EDFA), the pump pulses were injected into a 30-m PM fiber (FUT) through a circulator. Light at the other branch of the coupler was modulated by an SSBM, which worked at the lower-sideband output mode. One channel (CH1) of an AWG provided an RF signal with the form of (1), which drove the SSBM with the assistance of a 90° hybrid coupler. Another channel (CH2) of the AWG provided electrical pulses for EOM2, which was synchronized with CH1 to guarantee that each tone of the probe was amplified only by one pump pulse. The duration of modulation by each tone was 1.4 $\mu\varepsilon$, which was much longer than the round-trip propagation delay along the FUT. The probe trace was recorded by an oscilloscope.

The theoretical analysis in Part 2 has shown that the noise tones in the output spectrum of the SSBM can impose modulations on the BGS, the frequency of which varies with the position along the FUT. So firstly, this effect was studied and tested. In this experiment, there was no strain loaded on the FUT. The frequency of the arbitrary waveform changed from 200 MHz to 400 MHz with a step of 1 MHz. The frequency of the sinusoidal waveform was set to be 10.55 GHz. The measured BGS is shown in Fig. 4, where Fig. 4(a), (c), and (e) correspond to three different positions in the FUT (denoted as Position P1, P2, and P3, respectively). The distance between Position P1 and P2 is 20 ns in the echo trace, or ~2 m in the FUT, and the distance between P2 and P3 is 60 ns, or ~6 m in the FUT. Their amplitude spectra are calculated via FFT and shown in Fig. 4(b), (d) and (f), respectively. The FFT spectra show that the modulations are generated by two beat signals. One of them derives from the beat between the lower first-order sideband and the carrier, which is marked in black text and arrows in the panels. The modulation frequencies in Fig. 4(b), (d) and (f) are 135 ns, 155 ns, and 215 ns, respectively. The differences between them are respectively 20 ns and 60 ns, which are equal to the time difference as predicted. The other one is the beat between the lower and the upper first-order sideband, which is marked in red text and arrows. The modulation frequencies are respectively 270 ns, 310 ns, and 430 ns, twice the previous modulation frequencies. The experimental results are in good agreement with the theoretical model. Because the extinction ratios of the carrier and the upper first-order sideband of the SSBM vary with the frequency, the amplitude of modulation is not constant in Fig. 4.

In order to remove the modulations from the measured BGS profile, a 100-MHz low-pass filter which followed the detection of the output probe was employed to suppress the beat between the probe wave and noise tones. With the assistance of the filter, the BGS along the FUT was

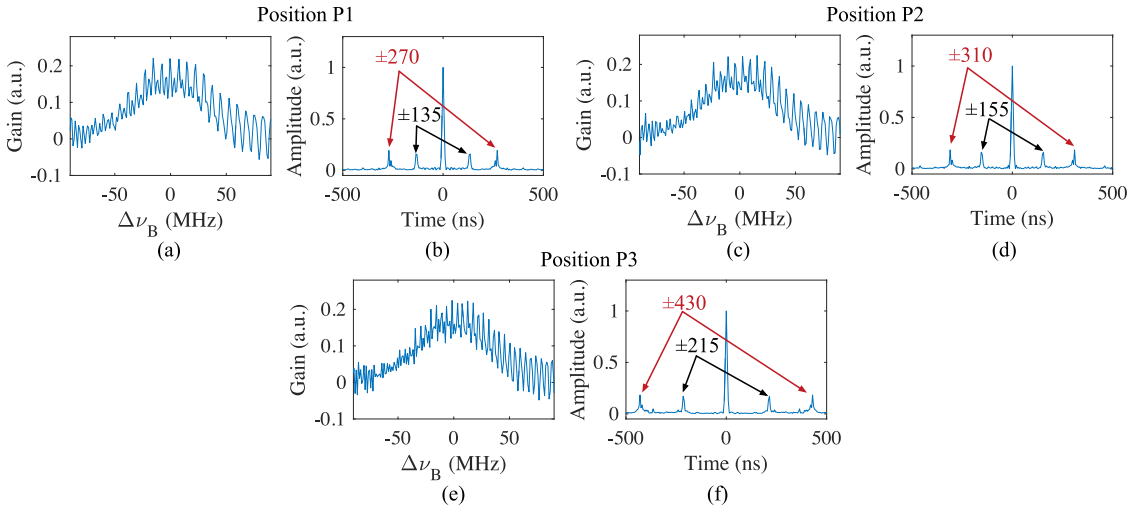

Fig. 4. Measured BGSs and their amplitude spectra. (a), (c), (e) BGSs of different positions in the FUT. The distance between Position P1 and P2 is 20 ns in the echo trace, or ~2 m in the FUT, and the distance between P2 and P3 is 60 ns. (b), (d), (f) FFT traces of (a), (c), and (e), respectively.

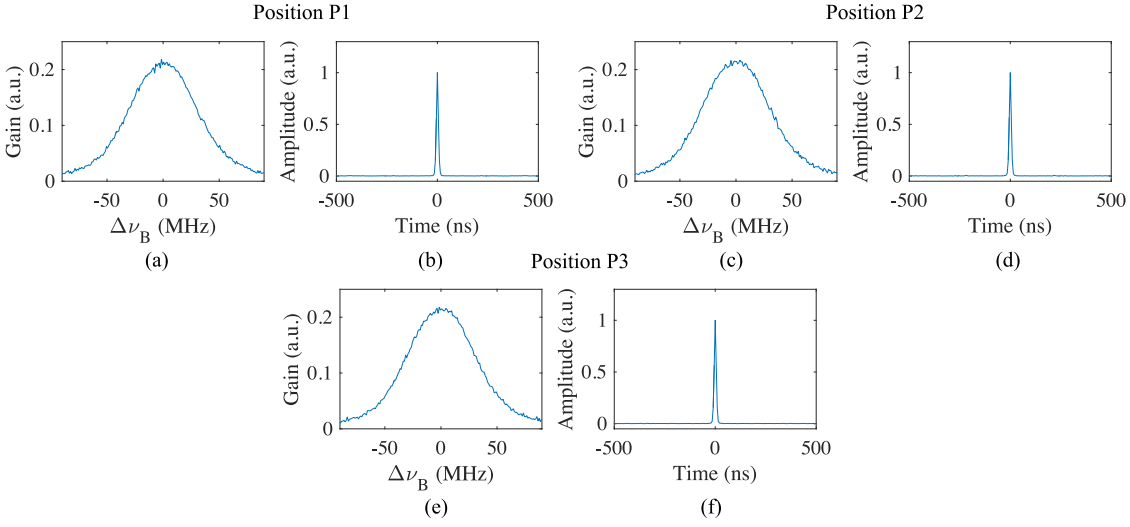

Fig. 5. Measured BGS when a low-pass filter is used to suppress the modulation on the BGS profile. The BGSs of the same points addressed in Fig. 4 are shown in (a), (c), and (e). (b), (d), (f) are Corresponding FFT spectra.

measured again. The BGSs of the same positions addressed in Fig. 4 are presented in Fig. 5. Similarly, we analyzed the amplitude spectra of the BGSs through FFT, the results of which are respectively shown in Fig. 5(b), (d), and (f), which suggest that the modulations on the BGS profile are effectively suppressed.

Next, two experiments of dynamic sensing based on dual-modulation were carried out. The frequency of the sinusoidal waveform was set to be 10.5 GHz, while the frequency of the arbitrary waveform was scanned from 200 MHz to 700 MHz with a step of 4 MHz, which enabled the scanning of the BGS to cover the range from 10.7 GHz to 11.2 GHz. In the first dynamic sensing experiment, a dynamic stretching was loaded via an off-axis plate driven by a DC motor. The dynamic change of the BGS was measured every 1 ms, the result of which is shown in Fig. 6. A moving average over

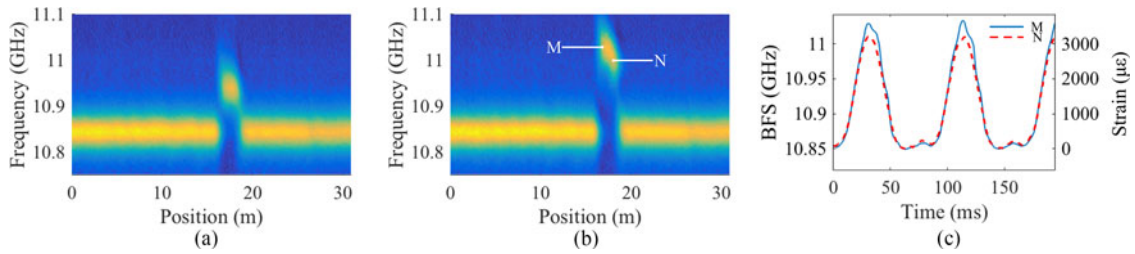

Fig. 6. Measured dynamic change of the BGS in the FUT. (a) BGS measured when t = 20 ms. (b) BGS measured when t = 32 ms. (c) BFS variation of two points (Point M and Point N) in the stretching section. Because of the fraction between the fiber and the off-axis plate, the strain of the left-half part of the stretching section is larger than that of the right-half. The corresponding BFSs are shown in blue and red curves, respectively.

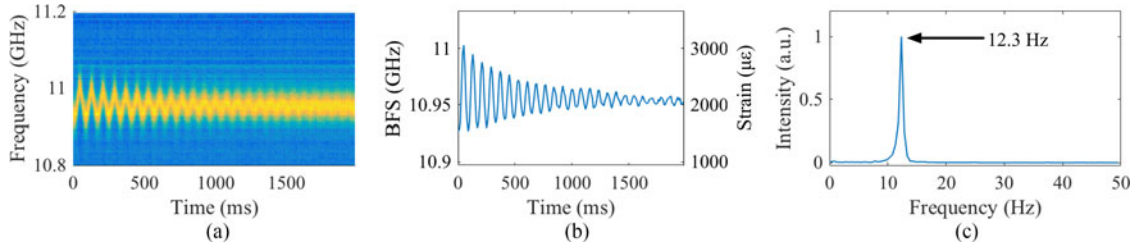

Fig. 7. Measured vibration of the fiber. (a) BGS of the vibration point. (b) BFS of the vibration point as a function of time. (c) Its power spectrum.

5-frame data was applied to improve the SNR. One frame of the BGS is drawn in Fig. 6(a), which corresponds to the 20th frame, showing that an ∼2-m segment of fiber was stretched. The BGS distribution when the strain reaches its maximum value in this experiment is shown in Fig. 6(b). The BFS is not even in the stretching section, which derives from the friction between the optical fiber and the off-axis plate. Because of the effect of the friction, the strain of the left-half part of the stretching section is larger than that of the right-half. The corresponding BFSs are shown in blue and red curves, respectively, in Fig. 6(c). The BFS varies from 10.85 GHz to 11.03 GHz, with a frequency of 11.8 Hz.

In the second experiment, vibrations were measured along the fiber. We pulled one point in the middle of a segment of fiber and then released it. The BGS was measured every 10 ms and 199 frames of data were recorded. The results are shown in Fig. 7 without data average. Damped oscillations are observed at a frequency of 12.3 Hz.

4. Conclusion

A dynamic sensor based on dual-modulation is proposed, in which the frequency agility is realized by the combination of a single-frequency modulation and a frequency-agility modulation. The bandwidth requirement for the AWG is reduced to several-hundred megahertz. Though a microwave generator is employed in the experiment, it is not essential. Because the frequency of the single-frequency modulation is constant, the ∼10-GHz-bandwidth microwave generator can be replaced by a sinusoidal wave generator with fixed frequency in practical application or product.

SSBM is central to the proposed method. Residual carrier and opposite sideband components at the SSBM output are unavoidable. The effects of these noise tones on the measurement of the BGS were verified in both theory and experiment. The research shows that modulations are imposed on the profile of the BGS due to the noise tones. It was effectively suppressed by a low-pass filter following the detection of the output probe. Finally, using an arbitrary waveform of 700-MHz bandwidth, two experiments of distributed dynamic sensing were carried out with 1-m

spatial resolution: 1) An 11.8-Hz strain-variation induced by the rotation of an off-axis plate was measured with a sampling rate of 200 Hz; 2) a damped vibration of the fiber was monitored with a sampling rate of 100 Hz.

Acknowledgment

The authors wish to thank Prof. A. Zadok, who helped revising the manuscript.

References

[1] T. Horiguchi, T. Kurashima, and M. Tateda, "Tensile strain dependence of Brillouin frequency shift in silica optical fibers," *IEEE Photon. J.*, vol. 1, no. 5, pp. 107–108, May 1989.
[2] D. Culverhouse, F. Farahi, C. N. Pannell, and D. A. Jackson, "Potential of stimulated Brillouin scattering as sensing mechanism for distributed temperature sensors," *Electron. Lett.*, vol. 25, no. 14, pp. 913–915, Jul. 1989.
[3] M. Tateda, T. Horiguchi, T. Kurashima, and K. Ishihara, "First measurement of strain distribution along field-installed optical fibers using Brillouin spectroscopy," *J. Lightw. Technol.*, vol. 8, no. 9, pp. 1269–1272, Aug. 1990.
[4] T. Kurashima, T. Horiguchi, and M. Tateda, "Distributed-temperature sensing using stimulated Brillouin-scattering in optical silica fibers," *Opt. Lett.*, vol. 15, no. 18, pp. 1038–1040, 1990.
[5] P. Chaube, B. G. Colpitts, D. Jagannathan, and A. W. Brown, "Distributed fiber-optic sensor for dynamic strain measurement," *IEEE Sens. J.*, vol. 8, no. 7, pp. 1067–1072, Jul. 2008.
[6] R. Bernini, A. Minardo, and L. Zeni, "Dynamic strain measurement in optical fibers by stimulated Brillouin scattering," *Opt. Lett.*, vol. 34, no. 17, pp. 2613–2615, Sep. 2009.
[7] Y. Peled, A. Motil, and M. Tur, "Fast Brillouin optical time domain analysis for dynamic sensing," *Opt. Exp.*, vol. 20, no. 8, pp. 8584–8591, 2012.
[8] J. Urricelqui, A. Zornoza, M. Sagues, and A. Loayssa, "Dynamic BOTDA measurements based on Brillouin phase-shift and RF demodulation," *Opt. Exp.*, vol. 20, no. 24, pp. 26942–26949, Nov. 2012.
[9] A. Bergman, L. Yaron, T. Langer, and M. Tur, "Dynamic and distributed slope-assisted fiber strain sensing based on optical time-domain analysis of Brillouin dynamic gratings," *J. Lightw. Technol.*, vol. 33, no. 12, pp. 2611–2616, Jun. 2015.
[10] I. Sovran, A. Motil, and M. Tur, "Frequency-scanning BOTDA with ultimately fast acquisition speed," *IEEE Photon. Technol. Lett.*, vol. 27, no. 13, pp. 1426–1429, Jul. 2015.
[11] A. Minardo, A. Coscetta, R. Bernini, and L. Zeni, "Heterodyne slope-assisted Brillouin optical time-domain analysis for dynamic strain measurements," *J. Opt.*, vol. 18, no. 2, Feb. 2016, Art. no. 025606.
[12] H. Lee, N. Hayashi, Y. Mizuno, and K. Nakamura, "Slope-assisted Brillouin optical correlation-domain reflectometry: Proof of concept," *IEEE Photon. J.*, vol. 8, no. 3, Jun. 2016, Art. no. 6802807.
[13] Y. Peled, A. Motil, L. Yaron, and M. Tur, "Slope-assisted fast distributed sensing in optical fibers with arbitrary Brillouin profile," *Opt. Exp.*, vol. 19, no. 21, pp. 19845–19854, 2011.
[14] A. Minardo, A. Coscetta, S. Pirozzi, R. Bernini, and L. Zeni, "Modal analysis of a cantilever beam by use of Brillouin based distributed dynamic strain measurements," *Smart Mater. Struct.*, vol. 21, no. 12, Dec. 2012, Art. no. 125022.
[15] A. Motil, O. Danon, Y. Peled, and M. Tur, "Pump-power-independent double slope-assisted distributed and fast Brillouin fiber-optic sensor," *IEEE Photon. Technol. Lett.*, vol. 26, no. 8, pp. 797–800, Apr. 2014.
[16] A. Minardo, G. Porcaro, D. Giannetta, R. Bernini, and L. Zeni, "Real-time monitoring of railway traffic using slope-assisted Brillouin distributed sensors," *Appl. Opt.*, vol. 52, no. 16, pp. 3770–3776, Jun. 2013.
[17] S. S. L. Ong and K. Hotate, "Dynamic strain measurement at 50 Hz using a Brillouin optical correlation domain analysis based on fiber optic sensor," in *Proc. 5th Pac. Rim Conf. Lasers Electro-Opt.*, vol. 2, 2003, p. 672.
[18] K. Y. Song and K. Hotate, "Distributed fiber strain sensor with 1-kHz sampling rate based on Brillouin optical correlation domain analysis," *IEEE Photon. Technol. Lett.*, vol. 19, no. 23, pp. 1928–1930, Dec. 2007.
[19] K. Y. Song, M. Kishi, Z. He, and K. Hotate, "High-repetition-rate distributed Brillouin sensor based on optical correlation-domain analysis with differential frequency modulation," *Opt. Lett.*, vol. 36, no. 11, pp. 2062–2064, Jun. 2011.
[20] Y. Mizuno, W. Zou, Z. He, and K. Hotate, "Proposal of Brillouin optical correlation-domain reflectometry (BOCDR)," *Opt. Exp.*, vol. 16, no. 16, pp. 12148–12153, Aug. 2008.
[21] Y. Mizuno, N. Hayashi, H. Fukuda, K. Y. Song, and K. Nakamura, "Ultrahigh-speed distributed Brillouin reflectometry," *Light Sci. Appl.*, vol. 5, 2016, Art. no. e16184.
[22] Y. Dong *et al.*, "High-spatial-resolution fast BOTDA for dynamic strain measurement based on differential double-pulse and second-order sideband of modulation," *IEEE Photon. J.*, vol. 5, no. 3, Jun. 2013, Art. no. 2600407.
[23] D. Ba *et al.*, "Distributed measurement of dynamic strain based on multi-slope assisted fast BOTDA," *Opt. Exp.*, vol. 24, no. 9, pp. 9781–9793, 2016.